Journal of Subsea and Offshore
-Science and Engineering-
July 1, 2026. Vol.17 No.1

Analyzed Mooring of Rounded-Shape FPSO using Lumped Method

Nur Aireen bt. Amran,[a], J. Koto,[a,b,*], Adibah Fatihah Mohd Yusof,[a], C. L. Siow,[a,]

[a)]*School of Mechanical Engineering, Universiti Teknologi Malaysia, Malaysia*
[b)]*Ocean and Aerospace Research Institute, Indonesia*

*Corresponding author: jaswar,koto@gmail.com and jaswar@utm.my

Paper History

Received: 22-November-2018
Accepted: 30-May-2026

ABSTRACT

Mooring line is functionally to maintain the position of floating structure under normal operating load and extreme storm load conditions. This paper discussed on mooring line of rounded-shape FPSO. Preparation procedures such as mooring design process and model setup were carried out. Mooring design process includes analysis displacement of taut mooring based on Lumped method. Simulation software based on the Lumped method was written in Visual Basic language called Finite Element on Mooring and Riser. The basin tank experiment also was conducted to study the hydrodynamic characteristic of the round-shape FPSO. In the experiment, the FPSO model is constructed based on scale ratio 1:110 and it is installed in wave dynamic tank with model size mooring lines.

KEY WORDS: *Rounded-Shape FPSO, Lumped Method, Model Experiment; Mooring Line.*

1.0 INTRODUCTION

Reduce of oil and gas resource in shallow water or onshore area forced the industry player to explore the resource to depth water area. Due to the increase of water depth, floating structures is more comparative compare to fix structure. Typically, the Floating Production Storage and Offloading, FPSO structure is converted from an old tanker ship but some of the FPSO owner is interest for new constructed hull. In term of system requirement, the FPSO is required better performance in stability either static or dynamic condition compare to resistance performance. This allows the FPSO to have simpler hull form compare to ship. Due to this point, several researchers conducted their study and design a new generation non-ship-shape FPSO and simulate the hydrodynamic characteristic of the FPSO by numerical or experimental method.

In year 2008, Lamport and Josefsson, (2008) carried a research to study the advantage of round shape FPSO over the traditional ship-shape FPSO [1]. The comparisons were made to compare motion response, mooring system design, constructability and fabrication, operability, safety and costing between both the structures. One of the finding on their study is their designed structures motions are similar for any direction of incident wave with little yaw excitation due to mooring and riser asymmetry. Next, Arslan, Pettersen, and Andersson (2011) are also performed a study on fluid flow around the round shape FPSO in side-by-side offloading condition. FLUENT software was used to simulate three dimensional (3D) unsteady cross flow pass a pair of ship sections in close proximity and the behavior of the vortex-shedding around the two bluff bodies [2]. Besides, simulation of fluid flow Characteristic around Rounded-Shape FPSO was also conducted by A. Efi et al. using RANs Method [3].

Also, Srinivasan et al (2008) proposed a non-ship-shaped circular FPSO concept which has a capability for round-the-year drilling and production operation within an Arctic Frontier Region [4]. The structure is designed to work in clear water open-sea and in ice-covered arctic environment with least ice-management requirement. The study on this new concept including ice-structure interaction, stability, storage, constant draft, motion, moon pool resonance, moorings and station keeping, flexible riser system, disconnect turret system, offloading operation, fabrication, transportation, and installation.

Besides, Wang, Zhang, and Liu (2012) were also proposed a non-ship-shape FPSO called inverted fillet quadrangular frustum pyramid-shaped FPSO (IQFP) [5]. The hydrodynamic characteristic of this structure was studied by using three-dimensional potential flow theory in frequency domain simulation. The obtained result was compared to ship-shaped FPSO with similar tonnage. The results indicate that the IQFP has large stability margin and better hydrodynamic performance than the ship-shaped FPSO. Siow et.al studied on motion responses of ship and rounded-shape FPSO [6-9]

Journal of Subsea and Offshore
-Science and Engineering-
July 1, 2026. Vol.17 No.1

2.0 MODELLING OF FPSO

In this study, the FPSO model and mooring lines in model scale are scaling follow the Froude similarity. Froude's law of similarity is the most appropriate scaling law applicable for the free and moored floating structure experiments. The Froude number has a dimension corresponding to the ratio of u^2/gD where u is the fluid velocity, g is the gravity acceleration and D is a length of the model or prototype. The Froude number Fr is defined as $Fr = u^2/gD$.

Let the subscripts p and m stand for prototype and model respectively and λ is the scale factor, then the scaling for length, speed, mass and force is shown in Table 1.

Table 1: Scaling law between model and prototype

Dimension	Scaling equation
length, l (m)	$l_p = \lambda l_m$
speed, u (m/s)	$u_p = \sqrt{\lambda} u_m$
mass, m (kg)	$m_p = \lambda^3 m_m$
Force, F (N)	$F_p = 1.025\lambda^3 F_m$
Mooring line stiffness in water, K (N/m)	$K_p = 1.025\lambda^2 K_m$

3.0 PRINCIPAL DIMENSION

In this study, the round shape FPSO model was designed and constructed to test in model experiment so the hydrodynamics characteristic of this designed model can be simulated. The round shape FPSO model was constructed based on full scale model where it diameter at designed draught is 112m. In the experiment, the round shape FPSO model was scaled down with ratio 1:110.

Upon the model complete constructed, few tests were carried out to ensure the model particulars is suited to the design. Firstly, inclining test and decay test were carried out to identify the hydrostatic particular for the round shape FPSO model. The Figure 1 showed the inclining test conducted before model experiment to check the vertical center of gravity of the structure. Besides, natural periods for the roll motions also obtained from decay test. The dimension for the models was summarized as in Table 2.

Table 2: Principal particulars of FPSO, scale 1/110.0

Symbol	Model Scale	Full Scale
Diameter (m)	1.018	111.98
Depth (m)	0.4401	48.41
Draught (m)	0.2901	31.91
Free board (m)	0.150	16.5
Displacement (m^3)	0.2361	314249
KG (m)	0.225	24.8
GM (m)	0.069	7.6

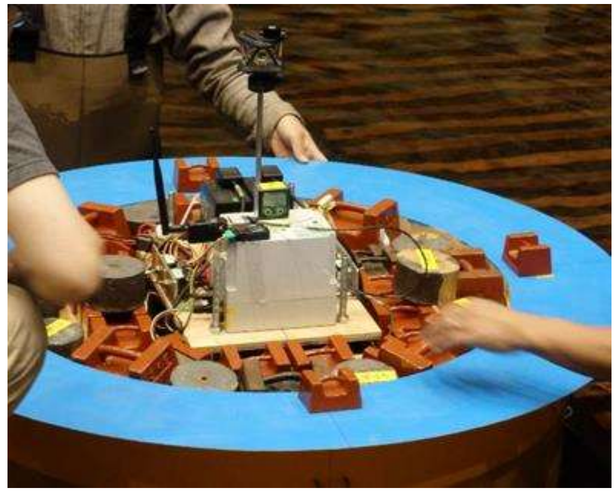

Figure 1: Inclining Test

5.0 MOORING LINES

In this experiment, four model scale mooring lines attached to the Round Shape FPSO to provide horizontal restoring force to the model. The mooring lines in full scale is designed by using the catenary theory and then scaled down to model scale follow by the scaling rule explained in section 2 of this paper [F]. The mooring line profile used in this experiment is showed in Figure 2 and the segment particular is showed in Table 3. The size of these mooring lines is pre-determined before the model experiment and the suitability of the mooring lines is analyzed using numerical simulation method to simulation the mooring performance in both static and dynamic condition.

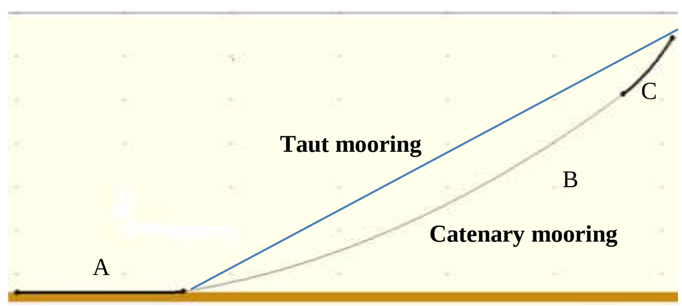

Figure 2: Catenary and taut mooring line profile

Also, due to the effect of mooring lines, the Round Shape FPSO will experience a non-linear horizontal restoring force during the experiment. The horizontal restoring force able to provide from the mooring lines to the FPSO model in order to return the FPSO back to the original position is showed in Figure 3.

Table 3: Mooring line segment information

Particular	Segment A	Segment B	Segment C
	Model	Model	Model
Nominal Diameter (mm)	3.0	3.0	3.0

JSOse | Received: 22-November-2018| Accepted: 30-May-2026| [(17) 1:1-9]
Published by International Society of Ocean, Mechanical and Aerospace Scientists and Engineers, www.isomase.org., ISSN: 2442-6415

ISOMAse
Journal of Subsea and Offshore
-Science and Engineering-
July 1, 2026. Vol.17 No.1

Type	Chain	Wire Rope	Chain
Segment Length (m)	4.0	9.4	1.4
Air Weight (kg/m)	0.16	0.0369	0.16
Water weight in water (kg/m) Model scale water density: 1000kg/m^3	0.1425	0.03119	0.1425
Breaking Load (KN)	10.79	5.40	10.79
Modulus Elasticity (GPa)	114.59	61.00	114.59

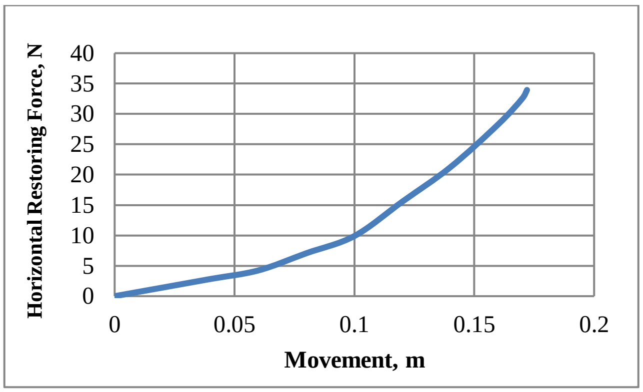

Figure 3: FPSO restoring force due to mooring effect.

4.0 MOORING LINE ANALYSIS

4.1 Lumped Method

Stress of mooring line is analyzed using lumped method based on spring theory. By using basic theory of spring method, the riser is modeled as a line, which is divided into a series of line segments as shown in Figure 13. The line segments only model the axial and torsional properties of the line. The other properties such as mass, weight, buoyancy, etc. are all lumped to the nodes. A simple lumped mass model of the riser is shown in Figure 4. The riser is discrete into N lumped mass nodes. Massless springs are used to connect nodes in consideration of the tangential elasticity of the line.

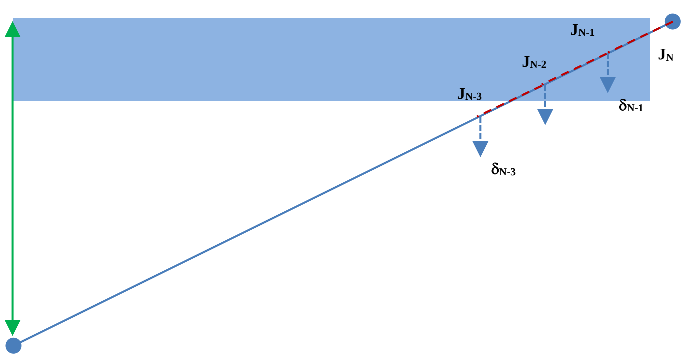

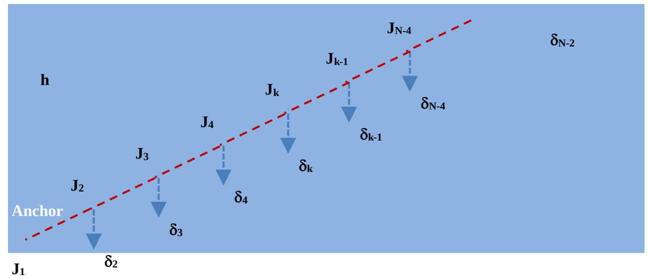

Figure 4: Application of lumped mass model of mooring line.

The force that spring experience will have to be same, otherwise the springs would buckle. Now by applying the famous hook's law, this means that

$$F = k\,x \qquad (1)$$

Where; F is external force, k is stiffness of riser, x is displacement.

The equations of forces for the j-th lumped mass node can be written in global coordinates. In order to solve the problem, one thing should be thought before creating the mathematical model which is about node-2. From figure below, node-2 is connected to both spring-1 and spring-2. Therefore, it would be experiencing forces from two springs and the force labeled as F_2 is the total force of the two component forces.

As shown in the Figure 5, since node-2 is influenced by two elastic forces which is one from spring-1 and other from spring-2, therefore total force on node-2 (F_2) can be described as follows:

$$F_2 = \underbrace{f_1^2}_{elastic\ force\ by\ spring-1\ acting\ on\ Node-2} + \underbrace{f_2^2}_{elastic\ force\ by\ spring-2\ acting\ on\ Node-2} \qquad (2)$$

By applying Equation.1, We can draw out four equations as follows.

$$\begin{cases} F_1 = k_1(x_1 - x_2) \\ f_1^2 = k_1(-x_1 + x_2), f_2^2 = k_2(x_2 - x_3) \\ f_2^2 = k_2(-x_2 + x_3), f_3^2 = k_3(x_3 - x_4) \\ f_3^2 = k_3(-x_3 + x_4), f_4^2 = k_4(x_4 - x_5) \\ F_5 = k_4(-x_4 + x_5) \end{cases} \qquad (3)$$

JSOse | Received: 22-November-2018| Accepted: 30-May-2026| [(17) 1:1-9]
Published by International Society of Ocean, Mechanical and Aerospace Scientists and Engineers, www.isomase.org., ISSN: 2442-6415

Journal of Subsea and Offshore
-Science and Engineering-
July 1, 2026. Vol.17 No.1

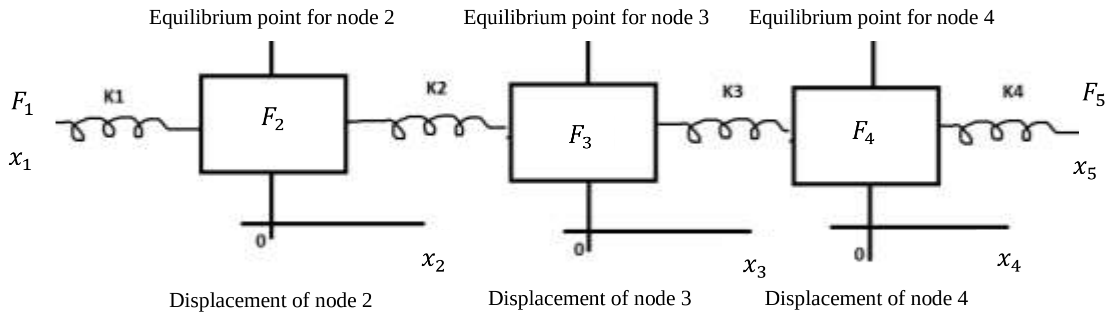

Figure 5: Simplification of finite element method on riser.

Since the two equations which is the second and third one is the force being applied to a single node (Node 2), we can combine the two equations n and as result we would finally have three equations as follows

$$\begin{cases} F_1 = k_1x_1 - k_1x_2 \\ F_2 = -k_1x_1 + (k_1+k_2)x_2 - k_2x_3 \\ F_3 = -k_2x_2 + (k_2+k_3)x_3 - k_3x_4 \\ F_4 = -k_3x_3 + (k_3+k_4)x_4 - k_4x_5 \\ F_5 = -k_4x_4 + k_4x_5 \end{cases} \quad (4)$$

Now we have a set of simultaneous equation comprised of 3 equations. 2-4. As it has already been seen above, a simultaneous equation can easily be converted into a matrix equation as follows

$$\begin{bmatrix} F_1 \\ F_2 \\ F_3 \\ F_4 \\ F_5 \end{bmatrix} = \begin{bmatrix} k_1 & -k_1 & & & \\ -k_1 & (k_1+k_2) & -k_2 & & \\ & -k_2 & (k_2+k_3) & -k_3 & \\ & & -k_3 & (k_3+k_4) & -k_4 \\ & & & -k_4 & k_4 \end{bmatrix} \begin{bmatrix} x_1 \\ x_2 \\ x_3 \\ x_4 \\ x_5 \end{bmatrix} \quad (5)$$

Figure 6 shows the lumped mass–spring configuration at the j-th node. The force on the j-th node contains line tensions T and T_{j-1}, the angles between segment and x-axis θ_j and θ_{j-1}, node gravity δ_j, drag forces f_{dxj} and f_{dzj}. The forces for j-th node can be written as Eq.6

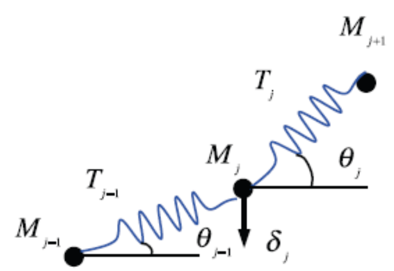

Figure 6: Lumped mass–spring configuration at j-th node.

$$\begin{bmatrix} F_{xj} \\ F_{zj} \end{bmatrix} = \begin{bmatrix} T_j\cos\theta_j - T_{j-1}\cos\theta_{j-1} - f_{dxj} \\ T_j\sin\theta_j - T_{j-1}\sin\theta_{j-1} - f_{dzj} - \delta_j \end{bmatrix} \quad (7)$$

Drag forces f_{dxj} and f_{dzj} may be derived from Morrison equations as follows

$$\begin{bmatrix} f_{dxj} \\ f_{dzj} \end{bmatrix} = \begin{bmatrix} -\frac{\rho}{2}D_c l\left(C_{dn}\sin\theta_j\,|u_{nj}|u_{nj} - C_{dt}\cos\theta_j\,|u_{tj}|u_{tj}\right) \\ \frac{\rho}{2}D_c l\left(C_{dn}\cos\theta_j\,|u_{nj}|u_{nj} - C_{dt}\sin\theta_j\,|u_{tj}|u_{tj}\right) \end{bmatrix} \quad (8)$$

$$\begin{bmatrix} u_{nj} \\ u_{tj} \end{bmatrix} = \begin{bmatrix} -(\dot{x}_j - c_j)\sin\theta_j + \dot{z}_j\cos\theta_j \\ (\dot{x}_j - c_j)\cos\theta_j + \dot{z}_j\sin\theta_j \end{bmatrix} \quad (9)$$

Where; C_{dn} and C_{dt} are the normal and tangential drag coefficients, respectively, and c_j is the current speed. The influence of marine growth needs to be considered in the definition of drag coefficients. They are assumed to increase linearly with growth thickness, which depends on operational measures as well as structural behavior.

$$\begin{bmatrix} F_1 \\ F_2 \\ F_3 \\ F_4 \\ F_{j-1} \\ F_j \end{bmatrix} = \begin{bmatrix} k_1 & -k_1 & & & & \\ -k_1 & (k_1+k_2) & -k_2 & & & \\ & -k_2 & (k_2+k_3) & -k_3 & & \\ & & -k_3 & (k_3+k_4) & -k_4 & \\ & & & -k_{j-2} & (k_{j-2}+k_{j-1}) & -k_{j-1} \\ & & & & -k_{j-1} & k_{j-1} \end{bmatrix} \begin{bmatrix} x_1 \\ x_2 \\ x_3 \\ x_4 \\ x_{j-1} \\ x_j \end{bmatrix} \quad (6)$$

JSOse | Received: 22-November-2018| Accepted: 30-May-2026| [(17) 1:1-9]
Published by International Society of Ocean, Mechanical and Aerospace Scientists and Engineers, www.isomase.org., ISSN: 2442-6415

ISOMAse

Journal of Subsea and Offshore
-Science and Engineering-
July 1, 2026. Vol.17 No.1

4.2. Oscillation Frequency

The $x(t)$ is displacement of cylinder can be written as

$$x(t) = A_x \sin(\omega_s t) \tag{10}$$

Where; A_x is the excitation amplitude of the cylinder.
Differentiation of the displacement (x) with respect to time, velocity ($\dot{x}$) and acceleration ($\ddot{x}$) can be written as

$$\dot{x} = \omega_s A_x \cos(\omega_s t)$$

$$\ddot{x} = -\omega_s{}^2 A_x \sin(\omega_s t). \tag{11}$$

The corresponding equation of oscillation for evaluating the response frequency of the system is given

$$(m + m_a)\ddot{x}(t) + kx(t) = 0$$

Inserted Eq.10 and Eq.11 into equation above, then this gives the still water response frequency of the cylinder:

$$-(m + m_a)\omega_s{}^2 A_x \sin(\omega_s t) + kA_x \sin(\omega_s t) = 0$$

$$(m + m_a)\omega_s{}^2 = k$$

$$\omega_s = 2\pi f_s = \sqrt{\frac{k}{(m+m_a)}}$$

$$f_s = \frac{1}{2\pi}\sqrt{\frac{k}{(m+m_a)}} \tag{12}$$

4.3. Motion of Mooring Line

The equations of motion for the j-th lumped mass node can be written in global coordinates as follows

$$\left(m_j + m_{aj}\right)\ddot{x}_j = F_j \tag{13}$$

Where; m_j is the mass matrix, m_{aj} is the added mass matrix, x_j is the displacement vector, and F_j is the external force.

Using the Figure 7, Equation 13 can be rewritten as follows

$$\left(m_j + A_{nj}\sin^2\theta_j + A_{tj}\cos^2\theta_j\right)\ddot{x}_j + \left(A_{tj} - A_{nj}\right)\ddot{z}_j \sin\theta_j \cos\theta_j = T_j\cos\theta_j - T_{j-1}\cos\theta_{j-1} - f_{dxj}$$

$$\left(m_j + A_{nj}\cos^2\theta_j + A_{tj}\sin^2\theta_j\right)\ddot{z}_j + \left(A_{tj} - A_{nj}\right)\ddot{x}_j \sin\theta_j \cos\theta_j = T_j\sin\theta_j - T_{j-1}\sin\theta_{j-1} - f_{dzj} - \delta_j \tag{14}$$

Where; A_{nj} and A_{tj} are the normal and tangential added mass, respectively; $\ddot{x}_j$ and $\ddot{z}_j$ are the acceleration of the j-th node at two directions.

In order to solve of the equations of motion in equation 10.8, the following initial and boundary conditions at the anchor position and displacement excitation at node-N should be introduced

$$x_0(t) = x_0,\ z_0(t) = z_0$$

$$x_N(t) = x_N,\ y_N(t) = z_N$$

$$x_i(0) = x_i^0,\ y_i(0) = z_i^0 \tag{15}$$

4.4 Displacement of Mooring Line

In the simulation, total pretension is 778 kN, elevation angle of mooring line is 13 degree and water depth 352 m as shown in Figure 7. Figure 8 show displacement of mooring for heave motion. The arrangement of mooring lines is shown in section 6.

Figure 7: Finite Element based Lumped Method

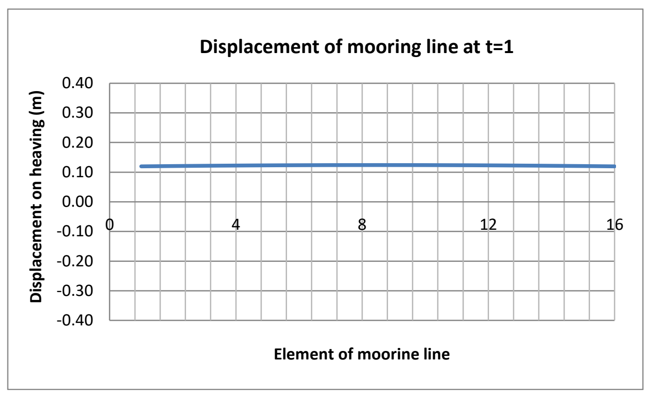

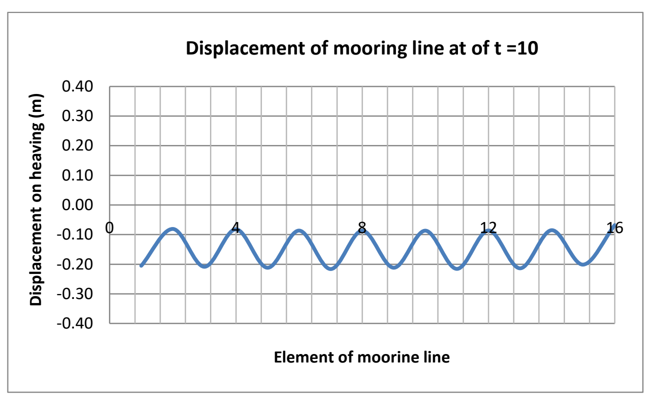

JSOse | Received: 22-November-2018| Accepted: 30-May-2026| [(17) 1:1-9]
Published by International Society of Ocean, Mechanical and Aerospace Scientists and Engineers, www.isomase.org., ISSN: 2442-6415

Journal of Subsea and Offshore
-Science and Engineering-
July 1, 2026. Vol.17 No.1

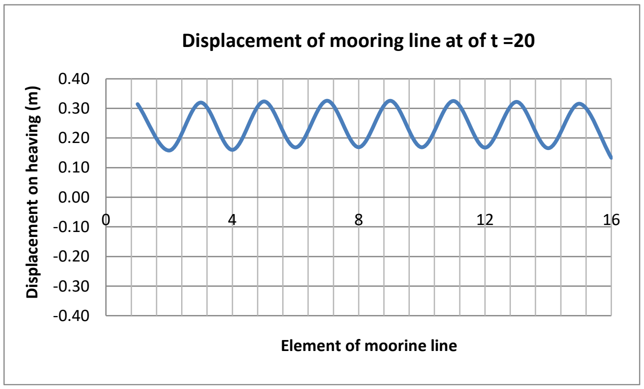

Figure 8: Displacement of taut mooring line in heave motion.

5.0 INSTRUMENT OF MODEL TEST

The round shape FPSO was assumed to experience six degrees of freedom during the experiment. The linear DOF motions of the FPSO models on model size mooring are measured by theodolite camera system (Figure 9a). The theodolite camera is able to capture the positions of the reflective optical tracking markers (Figure 9b) placed on the FPSO model automatically. The Rotational DOF motions of the FPSO models are measured by gyroscope (Figure 10) installed in the center of buoyancy of the FPSO.

(a)

(b)

Figure 9: Theodolite camera system to capture linear motion of FPSO model

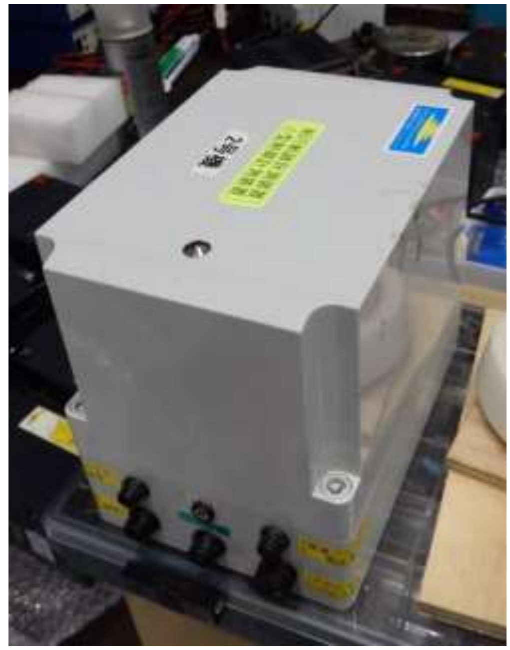

Figure 10: Gyroscope to capture model rotational motion of FPSO model.

A servo-type wave height measurement device (Servo 式波高計) as showed in Figure 11 is attached to the carriage which located at the position between FPSO model and wave generator to record the wave height generate by the wave generator.

Figure 11: servo-type wave height measurement device (Servo 式波高計) used to measure generated wave height.

All the measurement design is linked to separate computer to maximize the consistency of the measuring speed. To synchronize the device and ensure all device start and stop measure the data without delay, the Wireless remove controller as showed in Figure 12 is used to given the order to start and stop all measurement devices.

JSOse | Received: 22-November-2018| Accepted: 30-May-2026| [(17) 1:1-9]
Published by International Society of Ocean, Mechanical and Aerospace Scientists and Engineers, www.isomase.org., ISSN: 2442-6415

Journal of Subsea and Offshore
-Science and Engineering-
July 1, 2026. Vol.17 No.1

Figure 12: Wireless remove controller used to synchronize the start functioning and stop functioning of all measurement devices in the experiment.

6.0 EXPERIMENT OF FPSO

6.1 Experimental Setup

This experiment is conducted in wave dynamic tank with the length, wide and depth of 60m, 25m and 3.2m respectively. Before the experiment start, the Round FPSO model was fixed in the middle of tank by four mooring lines which connected between the fairleads located in bottom of FPSO with the anchors which sink into the bottom of tank. The position of the anchors and the arrangement of the mooring lines inside the tank are shown in Figure 13 and the view of FPSO model inside wave dynamic tank after installed with mooring lines is showed in Figure 14. Each anchor used in the experiment has the weight of 20kg in air.

Besides, to ensure the wave height measure by wave measuring device is not influence by the exist of Round FPSO, the carriage installed by the servo-type wave height measurement device is moved to the location between FPSO and wave generator where the distance between the FPSO to wave measuring device and the distance between wave generator to wave measuring device are 15m both.

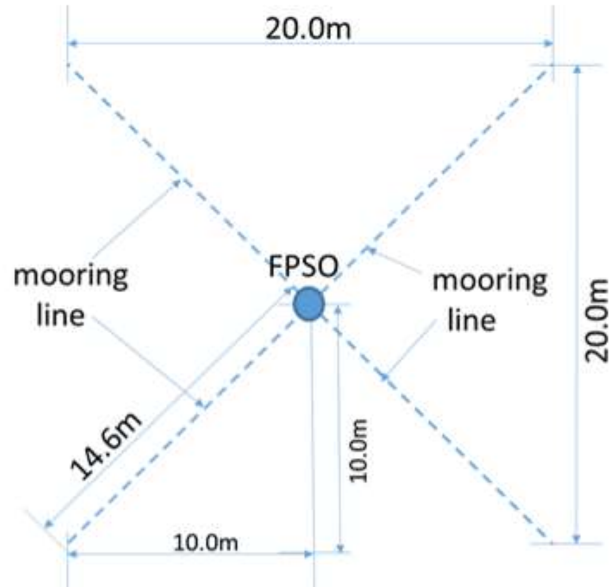

Figure 13: Arrangement of mooring lines and anchor in wave basin.

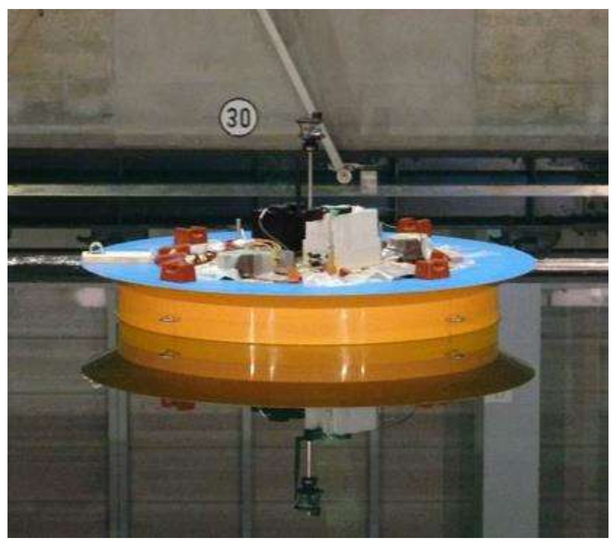

Figure 14: FPSO model fixed with mooring lines in wave basin in static condition.

6.2 Hydrodynamic of FPSO

In this study, the model experiment is conducted in head sea condition with the wave period in model scale from 0.7 seconds to 2.5 seconds and the wave height is 0.04m for all selected wave periods. The example of collected time domain motions data at wave period 1.7 seconds is presented in Figures 17 to 17. The Figure 15, Figure 16 and Figure 17 are presented the surge, heave and pitch motion of FPSO in time series collected from the model experiment.

JSOse | Received: 22-November-2018| Accepted: 30-May-2026| [(17) 1:1-9]
Published by International Society of Ocean, Mechanical and Aerospace Scientists and Engineers, www.isomase.org., ISSN: 2442-6415

ISOMAse
Journal of Subsea and Offshore
-Science and Engineering-
July 1, 2026. Vol.17 No.1

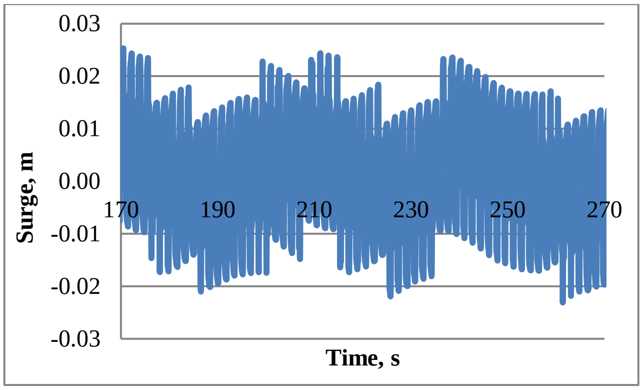

Figure 15: Surge motion time series data collected from model experiment at wave period 1.7s and wave height 0.04m.

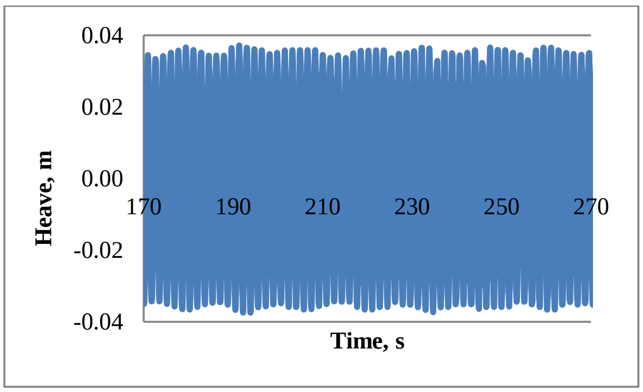

Figure 16: Heave motion time series data collected from model experiment at wave period 1.7s and wave height 0.04m.

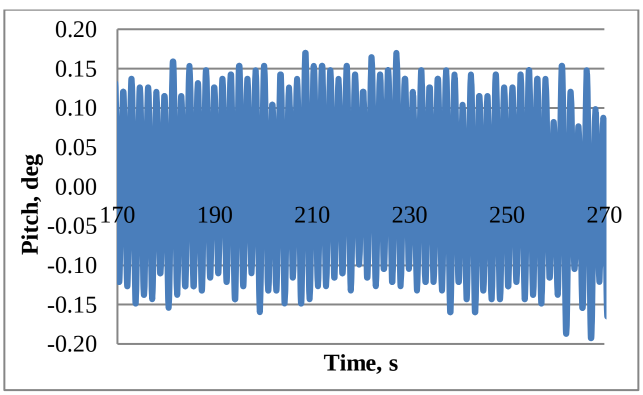

Figure 17: Pitch motion time series data collected from model experiment at wave period 1.7s and wave height 0.04m.

From Figure 15, it is shown that the surge motion experienced two types of motions at this wave period. First, the surge motion of FPSO model in this wave period is very depend on the wave frequency motion. Due to the effect of drift force and mooring lines, the FPSO also experienced slow varying motion and this can observe from the Figure 15. In Figure 15, the wave frequency motion is represented by the blue line while the slow varying motion can be obversed by link all peak points of blue line.

Compared to surge motion, heave and pitch motion is only experience the wave frequency motion. From the Figure 16 and 17, it is shown that the amplitude of heave and pitch motion are around 0.035m and 0.125degree. At this wave period, the heave motion is experience the resonance motion where the computed heave RAO by frequency domain calculation is around 1.7. Besides, the pitch motion amplitude calculated from the data also showed that the round FPSO model have good stability in the wave period 1.7s where the amplitude of pitch is only 0.125deg.

7.0 CONCLUSION

This paper presented the taut mooring of rounded-shape FFSO. Mooring line was analyzed based on displacement using Lumped method. Simulation software was written in Visual Basic language called Finite Element on Mooring and Riser. The basin tank experiment also was also conducted to study the hydrodynamic characteristic of the round-shape FPSO. In the experiment, the FPSO model is constructed based on scale ratio 1:110 and it is installed in wave dynamic tank with model size mooring lines.

ACKNOWLEGMENT

The authors are very grateful to Universiti Teknologi Malaysia, Hiroshima University, Japan, National Research Institute of Fisheries Engineering (NRIFE), Japan, Ocean and Aerospace Research Institute, Indonesia for supporting this study.

REFERENCES

1. Lamport, W. B. and Josefsson, P.M. (2008). The Next Generation Of Round Fit-For-Purpose Hull Form FPSOS Offers Advantages Over Traditional Ship-Shaped Hull Forms, *2008 Deep Gulf Conference*, December 9-11, New Orleans, Louisiana, USA.
2. Arslan, T., Pettersen, B. and Andersson, H.I. (2011). *Calculation of the Flow Around Two Interacting Ships*, Computational Methods in Marine Engineering IV, L.Eça, E. Oñate, J. García, T. Kvamsdal and P. Bergan (Eds.), pp. 254-265.
3. Afrizal, E., Mufti, F.M., Siow, C.L. and Jaswar. (2013). Study of Fluid Flow Characteristic around Rounded-Shape FPSO Using RANS Method. *The 8th International Conference on Numerical Analysis in Engineering*: 46 – 56. Pekanbaru, Indonesia.
4. Srinivasan et al. (2008). Design of Non-Ship-Shape FPSO for Sakhalin-V Deepwater, *SPE Russion Oil and Gas Technical Conference and Exhibition*, 28-30 October, Moscow, Russia.
5. Wang, T. Y., Zhang, J., and Liu, J. K. (2012*). Concept Design of a New Non-Ship-Shaped FPSO,* Applied Mechanics and Materials, Vol. 170-173, pp. 2222-2227.
6. Siow, C. L., Jaswar, K, and Khairuddin, N.M. (2014). *Study on Model Scale Rounded-Shape FPSO's Mooring Lines*,

JSOse | Received: 22-November-2018| Accepted: 30-May-2026| [(17) 1:1-9]
Published by International Society of Ocean, Mechanical and Aerospace Scientists and Engineers, www.isomase.org., ISSN: 2442-6415

Journal of Ocean, Mechanical and Aerospace Science and Engineering, Vol. 12, pp.1-6.

7. C. L. Siow, J. Koto, H. Yasukawa, A. Matsuda, D. Terada, C. Guedes Soares, Muhamad Zameri bin Mat Samad, 2014, Experiment Study on Hydrodynamics Characteristic of Rounded- Shape FPSO, *The 1st Conference on Ocean, Mechanical and Aerospace -science and engineering-*. Pekanbaru, Indonesia.
8. Siow, C.L., Koto, J., Yasukawa, H., Matsuda, A., Terada, D., Soares, C.G., Incecik, A., Pauzi, M.A.G. (2015). *Mooring Effect on Wave Frequency Response of Round Shape FPSO*. Jurnal Teknologi, Vol 74, No 5, pp.59-68
9. Siow, C.L., Koto, J., Yasukawa, H., Matsuda, A., Terada, D., Abyn, H. (2016). *Investigation Motion Responses of Ship Shape Floating Structure using Diffraction Potential*. Journal of Subsea and Offshore -Science and Engineering-, Vol.5
10. Koto, J., Siow, C. L., Khairuddin, Afrizal, N. M., Abyn, H., Soares, C. G. 2014. Comparison of Floating Structures Motion Prediction between Diffraction, Diffraction-viscous and Diffraction-Morison Methods. *The 2nd International Conference on Maritime Technology and Engineering*. Lisboa, Portugal.
11. Siow, C.L, Koto, J, Abby, H. Khairuddin, N.M, 2014, *Prediction of semi-submersible's motion response by using diffraction potential theory and heave viscous damping correction*, Jurnal Teknologi (Sciences and Engineering), Vol.69, No.7, 2014, pp.127-133.

JSOse | Received: 22-November-2018| Accepted: 30-May-2026| [(17) 1:1-9]
Published by International Society of Ocean, Mechanical and Aerospace Scientists and Engineers, www.isomase.org., ISSN: 2442-6415